

Cesar B. Rocha¹, Sarah T. Gille¹, Teresa K. Chereskin¹, and Dimitris Menemenlis²

Contents of this file

1. Text S1 with details of the LLC simulations.
2. Figure S1 with spectra of LLC2160 and LLC4320 simulations.
3. Table S1 with details about the LLC spin-up.
4. Figure S2 with time series of vorticity and divergence probability density functions.
5. Figure S3: root-mean-squares of vorticity, strain rate, and divergence as a function of depth.

Corresponding author: Cesar B. Rocha, Scripps Institution of Oceanography, University of California San Diego, La Jolla, CA, USA. (crocha@ucsd.edu)

¹Scripps Institution of Oceanography,
University of California San Diego, La Jolla,
CA, USA

²Earth Sciences Division, Jet Propulsion
Laboratory, California Institute of
Technology, Pasadena, CA, USA

6. Figure S4 with comparison of Argo climatological upper-ocean stratification and the LLC simulations
7. Text S5 with details about the comparison of model and mooring kinetic energy frequency spectra.
8. Figure S5: comparison of upper-ocean kinetic energy frequency spectra with spectra from available moored current meters.
9. Figure S6 showing the seasonal variations of the near-surface amplitude of the vertical modes.
10. Figure S7 Wavenumber-frequency spectrum of KE for LLC4320 simulation.

Introduction

This document contains supporting information with details regarding the model simulations, comparisons with observations, and supplemental figures.

S1: Detail of the LLC simulations

Table 1 shows details of the LLC spin-up hierarchy. Both simulations analyzed in the present paper, LLC2160 and LLC4320, were forced by surface fluxes from the 0.14° European Centre for Medium-range Weather Forecasting (ECMWF) atmospheric operational model analysis, starting in 2011, and the 16 most significant tidal components. The LLC code and model configuration files are available online (at http://mitgcm.org/viewvc/MITgcm/MITgcm_contrib/ llc_hires). The model output can be obtained from the ECCO project (http://ecco2.org/llc_hires).

For the LLC hierarchy, the sea-surface height is calculated using a linearized equation. While the nominal horizontal resolution of the LLC4320 and LLC2160 simulations are

$1/48^\circ$ and $1/24^\circ$, horizontal wavenumber spectra suggests an effective resolution of about 8 km and 20 km, respectively (see figure S1).

The spin-up of the upper-ocean in the LLC4320 ($1/48^\circ$) simulation is a couple of days, as depicted the time series of surface horizontal divergence in Figure 2b of the main text (see initial rapid increase in RMS divergence in September 2011). To avoid the spin-up stage, we chose October to characterize the late summer/early fall. The late winter/early spring waves chosen to be 6 months out-of-phase with late summer/early fall (hence April).

S5: How well do the LLC simulations capture high-frequency modes?

To assess how well the LLC simulations represents the high-frequency variability, we compare the model near-surface velocity field against two available mooring data records: KEO (the data are available online at <http://www.pmel.noaa.gov/ocs/KEO>) and KESS mooring #7 (the data are available online at <http://uskess.whoi.edu>). For proper comparison, we use model data closest to these two moorings (west of the region considered in the present study). Focusing on high-frequencies, we calculate frequency spectral estimates every month. There are about 48 independent spectral realizations.

Figure S5 shows KE frequency spectra for the LLC simulations and mooring data. At the uppermost common depth (20 m), very low frequencies (periods > 10 days) and the inertial, diurnal, and semi-diurnal frequencies agree well — the KESS data are more energetic at intermediate frequencies. At 40 m, the LLC simulations and observations have consistent spectra at periods larger than about 6 h. The data from the moorings are more energetic at higher frequencies, except for the first two harmonics that are apparent in the KESS data at 40 m. There are at least two reasons for the slightly more energetic super-

inertial variability in the observations: 1) The high- frequency variability is dominated by high-frequency noise due to mooring vertical excursions; and 2) The model does not have enough resolution to resolve the full internal wave spectrum.

References

- Levitus, S., J. Antonov, O. K. Baranova, T. Boyer, C. Coleman, H. Garcia, A. Grodsky, D. Johnson, R. Locarnini, A. V. Mishonov, et al. (2013), The world ocean database, *Data Science Journal*, 12(0), WDS229–WDS234.
- Rocha, C. B., T. K. Chereskin, S. T. Gille, and D. Menemenlis (2016), Mesoscale to submesoscale wavenumber spectra in Drake Passage, *Journal of Physical Oceanography*, 46, 601–620.
- Roemmich, D., and J. Gilson (2009), The 2004–2008 mean and annual cycle of temperature, salinity, and steric height in the global ocean from the Argo Program, *Progress in Oceanography*, 82(2), 81–100.

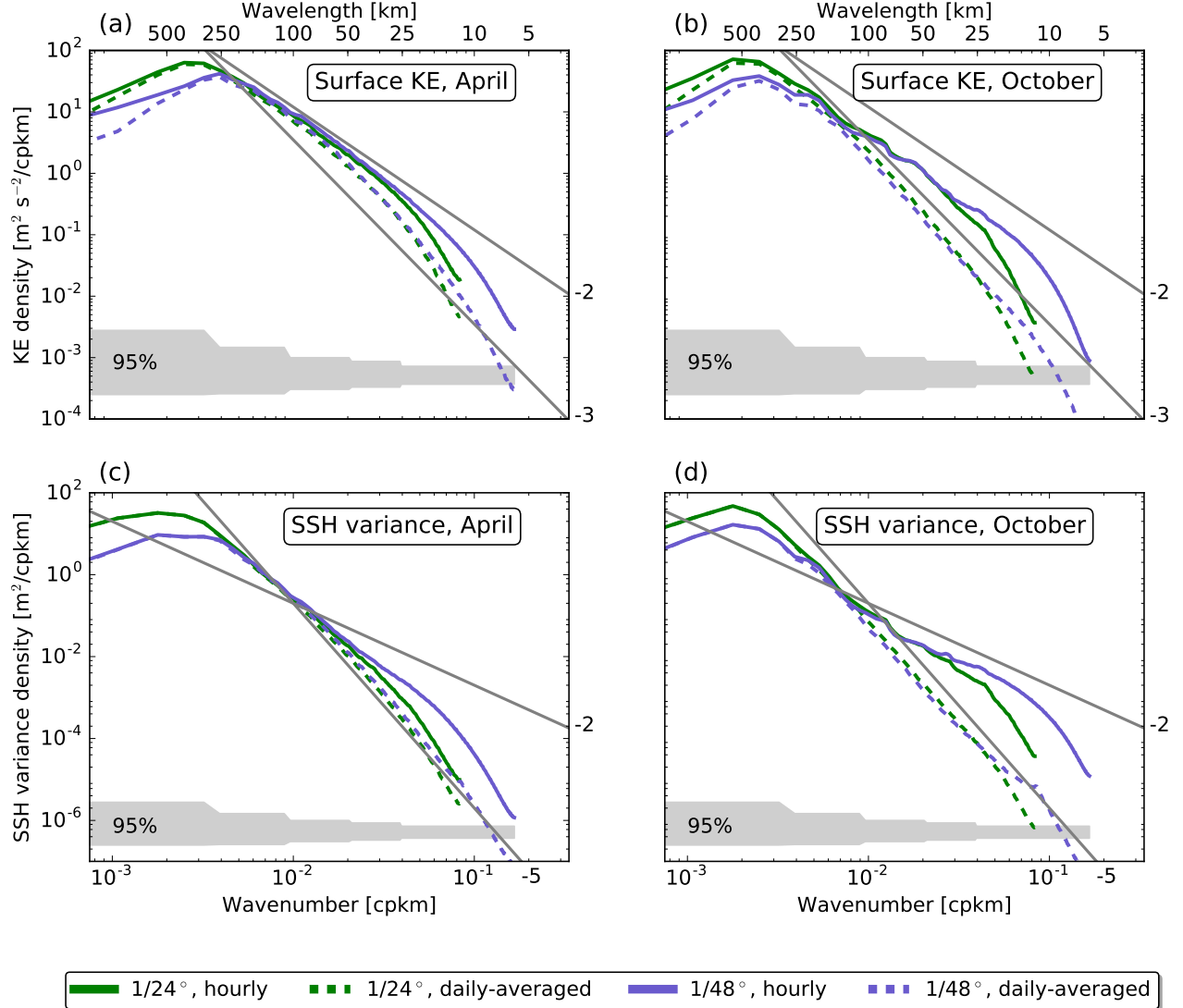


Figure S1. Comparison between spectra of the 1/24° (green) and 1/48° (purple) LLC simulations. The statistical error bars represent conservative 95% significance levels. As expected the higher-resolution simulation (LLC4320) essentially extends the spectra of the lower-resolution simulation (LLC2160) towards smaller scales, demonstrating that the higher resolution is resolving a wider array of scales. Between 20 and 100 km the spectra of the two simulations are visually indistinguishable.

Table S1. The MITgcm Latitude-Longitude Cap (LLC) spin-up hierarchy. This study analyzes the output of LLC2160 and LLC4320. Model fields are available hourly. Adapted from *Rocha et al. [2016]*.

| Simulation | Grid spacing | Time-step | Period | Tides |
|---------------|--------------|-----------|-------------------------------|-------|
| ECCO2 Adjoint | 18 km | 1200 s | January 2009 - December 2011 | No |
| LLC 1080 | 1/12° | 90 s | January 2010 - June 2012 | Yes |
| LLC 2160 | 1/24° | 45 s | January 2011 - April 2013 | Yes |
| LLC 4320 | 1/48° | 25 s | September 2011 - October 2012 | Yes |

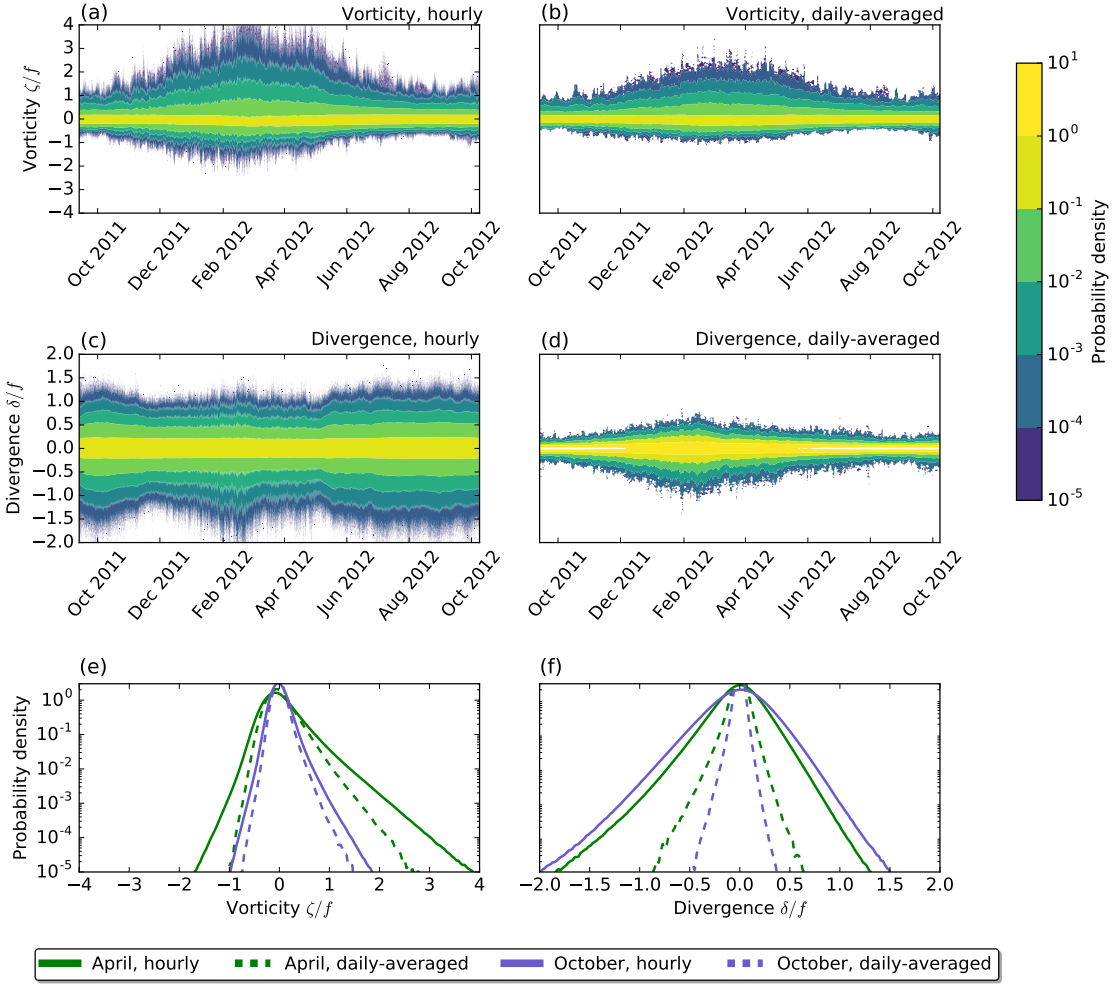


Figure S2. Time dependence of probability density functions of vertical vorticity (a, b) and horizontal divergence (c, d). Monthly averages in April and October are also shown (e, f). The time series of vorticity PDF indicate that the development of positive skewness in winter (Figures S3a-b) both in hourly (~ 1.4) and daily-averaged (~ 1.1) fields. The skewness in divergence for hourly fields is very small year-round (~ -0.24), suggesting the prevalence of inertia-gravity waves. Filtering out the waves by daily-averaging the velocity field increases the skewness in divergence, particularly in winter (~ -0.64). Both positive vorticity (cyclonic) skewness and negative divergence (convergence) skewness are characteristics of submesoscale turbulence.

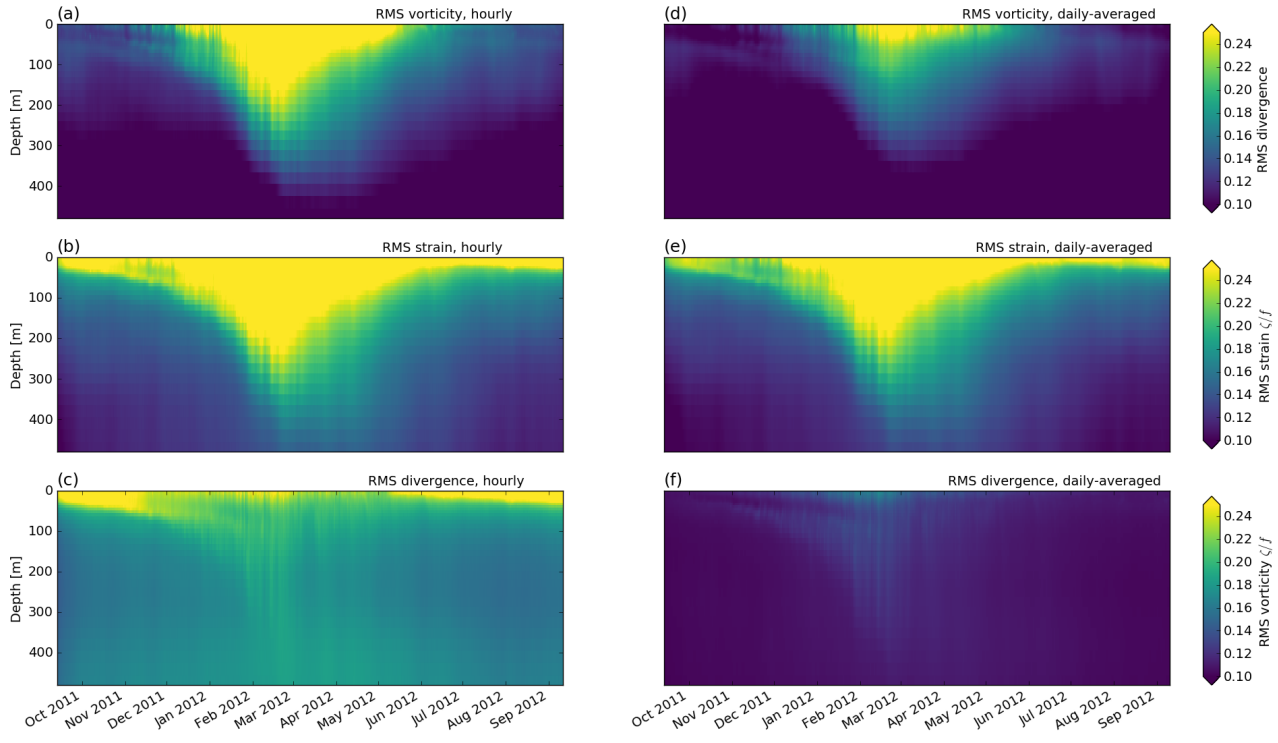


Figure S3. Depth-dependence of root-mean-square of vertical vorticity (a,d), rate of lateral strain (b,e) and horizontal divergence (c,f) for hourly (a,b,c) and daily-averaged (d,e,f,) fields. The strong seasonality, as depicted at the surface in Figure 2 of the main manuscript, is confined to the mixed layer, which varies from 50 m in summer to about 350 m in winter.

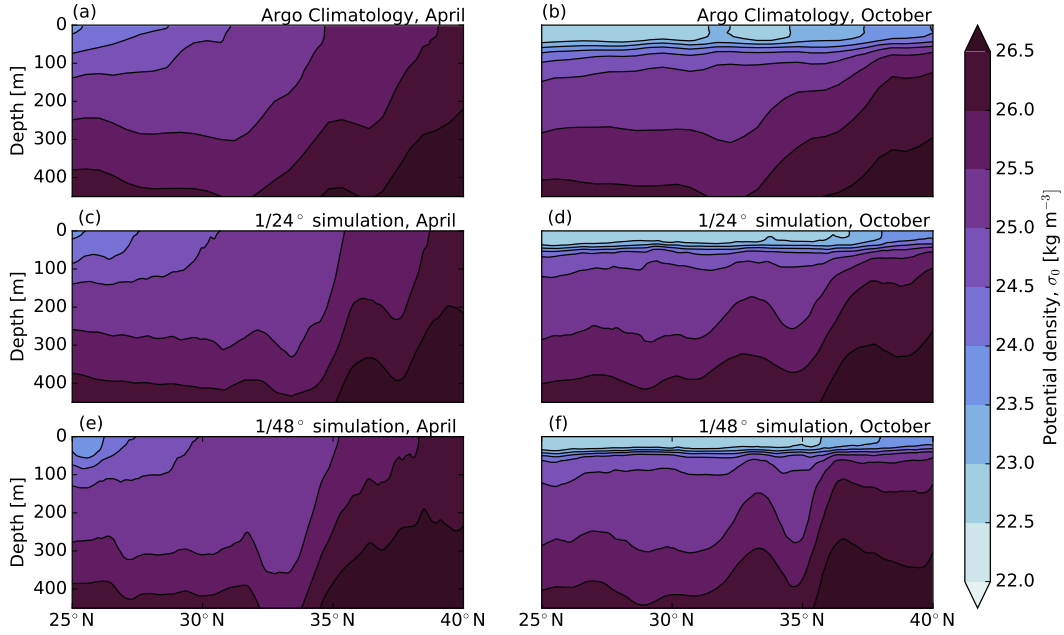


Figure S4. Potential density: a comparison between Roemmich-Gilson Argo climatology [updated from *Roemmich and Gilson [2009]*] (a, b) and the $1/24^\circ$ (c, d) and $1/48^\circ$ (e, f) LLC simulations. The Argo climatology is smoother owing to lower resolution and long-term averaging. Nonetheless, simulations reproduce the strong seasonality in the stratification. The upper ocean is weakly stratified in late winter/early fall and re-stratifies in summer. Argo climatology and LLC simulations mixed-layer depths are consistent during all seasons (not shown). The Argo climatology is available online at http://sio-argo.ucsd.edu/RG_Climatology.html.

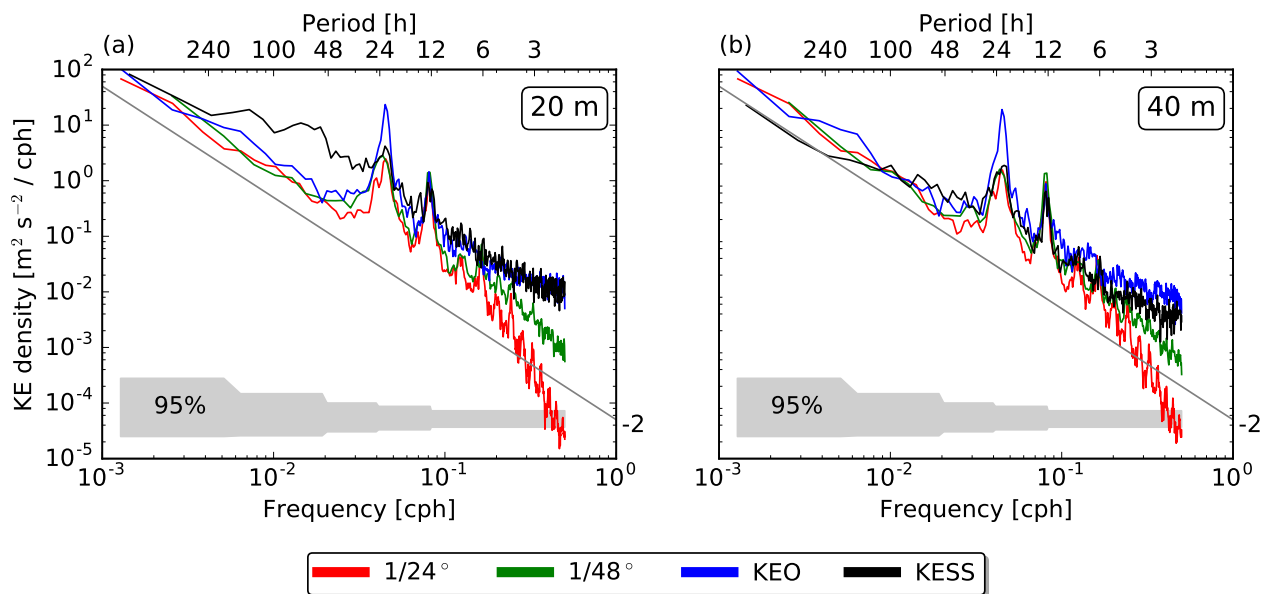


Figure S5. Comparison between frequency spectra of LLC simulations and two available moored current meter records.

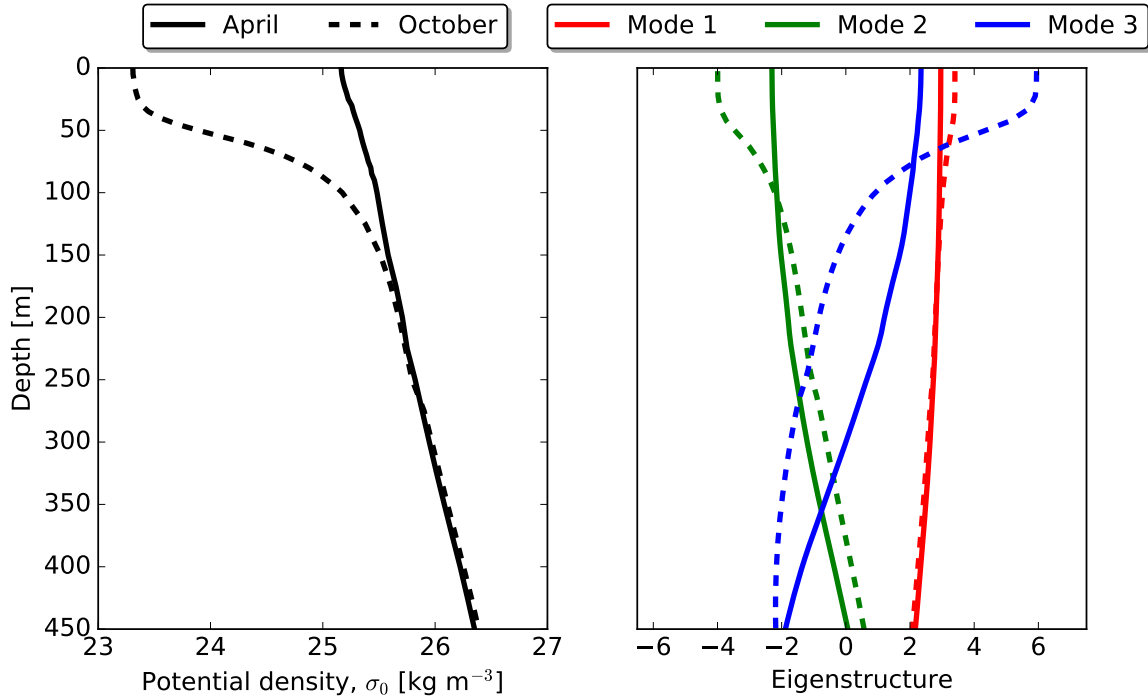


Figure S6. The seasonal variability of the WOA 2013 [Levitus *et al.*, 2013] stratification averaged over the domain and the associated three gravest pressure modes. Only the upper 450 m is shown. Clearly, the changes to the stratification are dramatic, with the formation of a seasonal pycnocline in summer. The strong seasonality of upper-ocean stratification yields a strong seasonality in the near-surface shape and amplitude of baroclinic pressure modes. In particular, the surface amplitude is much larger in summer. Thus the projection of baroclinic tides on the surface may have significant seasonal variations. The WOA data is available online at <https://www.nodc.noaa.gov/OC5/woa13/>.

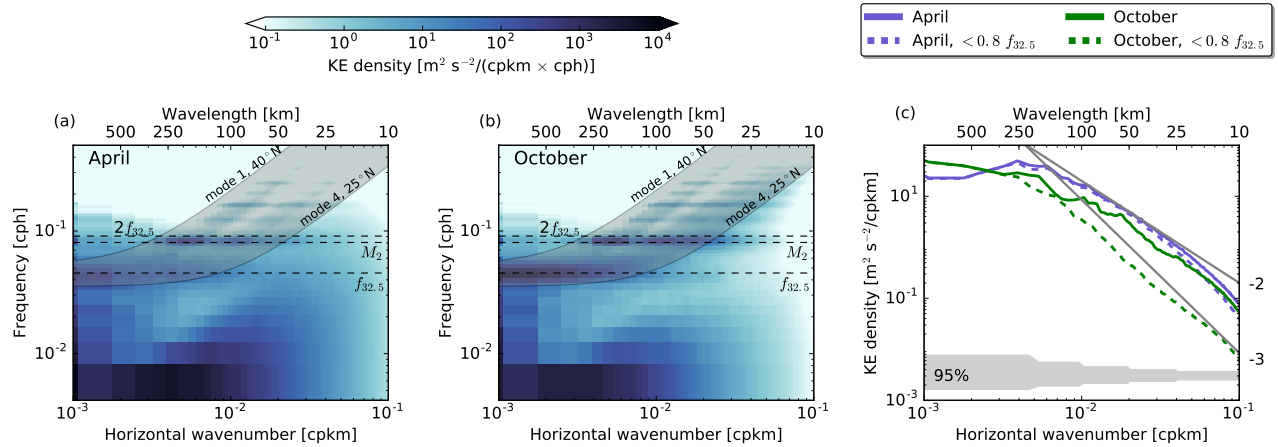


Figure S7. LLC4320 Wavenumber-frequency spectrum of KE in (a) April and (b) October.

(c) Wavenumber spectrum of SSH variance – the integral of (a) and (b) over frequency. In (a) and (b), the light gray shaded region depicts the dispersion relations for inertia-gravity waves from mode 1 through mode 4 across the latitudinal domain; horizontal dashed lines represent the semi-diurnal lunar tidal frequency (M_2), and the inertial frequency at mid-latitude ($f_{32.5}$) and its first harmonic ($2f_{32.5}$).